RESEARCH ARTICLE

Disease Models & Mechanisms 6, 146-159 (2013) doi:10.1242/dmm.009852

Glafenine-induced intestinal injury in zebrafish is ameliorated by μ-opioid signaling via enhancement of Atf6-dependent cellular stress responses

Jason R. Goldsmith[1], Jordan L. Cocchiaro[2], John F. Rawls[2,3,*,‡] and Christian Jobin[1,3,4,*,‡]

SUMMARY

Beside their analgesic properties, opiates exert beneficial effects on the intestinal wound healing response. In this study, we investigated the role of μ-opioid receptor (MOR) signaling on the unfolded protein response (UPR) using a novel zebrafish model of NSAID-induced intestinal injury. The NSAID glafenine was administered to zebrafish larvae at 5 days post-fertilization (dpf) for up to 24 hours in the presence or absence of the MOR-specific agonist DALDA. By analysis with histology, transmission electron microscopy and vital dye staining, glafenine-treated zebrafish showed evidence of endoplasmic reticulum and mitochondrial stress, with disrupted intestinal architecture and halted cell stress responses, alongside accumulation of apoptotic intestinal epithelial cells in the lumen. Although the early UPR marker BiP was induced with glafenine-induced injury, downstream *atf6* and *s-xbp1* expression were paradoxically not increased, explaining the halted cell stress responses. The μ-opioid agonist DALDA protected against glafenine-induced injury through induction of *atf6*-dependent UPR. Our findings show that DALDA prevents glafenine-induced epithelial damage through induction of effective UPR.

INTRODUCTION

Intestinal homeostasis is achieved in part by the maintenance of a functional barrier composed of a single layer of intestinal epithelial cells (IEC), which separates the host from the highly antigenic lumenal milieu (Sartor, 2008). Events leading to compromised barrier function are associated with various intestinal disorders including inflammatory bowel diseases (IBD) (Williams et al., 2001; Sartor, 2008). Conditions leading to an impaired mucosal barrier function are diverse and include medications (non-steroidal anti-inflammatory drugs or NSAIDs) (Morteau et al., 2000), radiation exposure (Packey and Ciorba, 2010), ischemic episodes (Kinross et al., 2009) and genetic predisposition (Sartor, 2008). Notably, genes that disrupt the unfolded protein response (UPR) and autophagy following cellular stress have recently been implicated in the pathogenesis of IBD (Kaser et al., 2010; Stappenbeck et al., 2011). The disease etiology remains unclear; however, genetic evidence and experimental models suggest that intestinal cell death due to improper responses to endoplasmic reticulum (ER) stress leads to impaired barrier function (Kaser et al., 2008). Because of the importance of the epithelium in maintaining intestinal homeostasis, understanding mechanisms involved in intestinal epithelial healing and cell stress responses, and the identification of compounds that promote these processes, could lead to new therapeutic strategies for IBD.

Epithelial barrier damage triggers a host response termed 'restitution/wound-healing' (Karrasch and Jobin, 2009). In this response, cells at the wound edge migrate into the wounded area, undergo cytoskeletal rearrangement and finally re-establish tight junction barriers with their neighboring cells (Karrasch and Jobin, 2009; Marchiando et al., 2011). This initial phase does not require epithelial proliferation, but renewal of cells are needed to replenish the decreased enterocyte pool after injury (Karrasch and Jobin, 2009). Various pathways including nuclear factor kappa-light-chain-enhancer of activated B cells (NF-κB), mitogen-activated protein kinase (MAPK), signal transducer and activator of transcription 3 (STAT3), glycogen synthase kinase-3β (GSK3β)/β-catenin (Kim and Jobin, 2010) and phosphatidylinositol 3-kinase (PI3K)/Akt (Karrasch and Jobin, 2009) are involved in the wound healing response through a combination of pro-migratory, proliferative and/or anti-apoptotic activities. The μ-opioid receptor (MOR) ligand DALDA has also recently been shown to activate the intestinal wound healing response in mice (Goldsmith et al., 2011). However, the mechanism of MOR-mediated protection is largely unknown at this point.

The wide array of upstream signals and downstream pathways has made the study of restitution/wound healing a complex and difficult area of research (Karrasch and Jobin, 2008; Karrasch and Jobin, 2009). The vast majority of our information on this complex process is derived from rodent models, which have limited capacity for imaging techniques and therapeutic investigation (Wirtz et al., 2007). Zebrafish (*Danio rerio*) possess several features that make it an attractive model for in vivo investigation of intestinal injury. Zebrafish are transparent through early adulthood, allowing the use

[1]Department of Pharmacology, University of North Carolina, Chapel Hill, NC 27599, USA
[2]Department of Cell and Molecular Physiology, University of North Carolina, Chapel Hill, NC 27599, USA
[3]Department of Microbiology and Immunology, University of North Carolina, Chapel Hill, NC 27599, USA
[4]Department of Medicine, University of North Carolina, Chapel Hill, NC 27599, USA
*These authors contributed equally to this work
‡Authors for correspondence (jfrawls@med.unc.edu; job@med.unc.edu)

Received 11 March 2012; Accepted 6 August 2012

TRANSLATIONAL IMPACT

Clinical issue

Damage to the intestinal epithelium is involved in numerous intestinal pathologies, such as ischemia-reperfusion injury, radiation injury and inflammatory bowel diseases (IBDs). Study of the mechanisms involved in intestinal injury and wound healing, and the development of therapeutics designed to enhance intestinal epithelial wound healing, are limited by the paucity of appropriate model systems. Currently available experimental platforms use rodent models with significant associated costs and time constraints. Zebrafish are an attractive alternative model organism for such studies: they have a digestive system similar to that of mammals, their optical transparency allows for the use of powerful in vivo imaging modalities, and their small size permits high-throughput genetic and chemical tests.

Results

Among many proposed agents that cause injury to intestinal epithelial cells (IECs) are non-steroidal anti-inflammatory drugs (NSAIDs). Here, the authors developed a larval zebrafish model of intestinal injury by administering the NSAID glafenine to zebrafish for up to 12 hours. The resulting pathology is characterized by rapid (within 1 hour of drug administration) IEC apoptosis that leads to sloughing of the cells into the intestinal lumen. Ultra-structure analysis showed that the IECs of glafenine-injured fish showed signs of endoplasmic reticulum (ER) stress and atypical, halted cell stress responses. The sloughing cells form a visible 'tube' of material, which can be labeled using the vital dye AO. Using a rapid assay to detect the presence of this tube, the authors screened several compounds for amelioration of IEC apoptosis. Of interest, the μ-opioid receptor (MOR) agonist DALDA markedly reduced tube formation. Further studies demonstrated that DALDA treatment drastically reduced IEC apoptosis and restored proper organelle stress responses. Finally, knockout of the autophagy gene *atf6* resulted in loss of DALDA protection, suggesting that DALDA protects from glafenine-mediated intestinal injury by inducing an *atf6*-dependent unfolded protein response (UPR).

Implications and future directions

This work establishes the first model of larval zebrafish intestinal injury, and shows that it can be used to screen for compounds that protect against it. Additionally, the glafenine-induced injury model recapitulates the recently discovered relationship between improper organelle stress responses and IEC apoptosis in another organism, demonstrating conservation of this phenomenon across species. Finally, this work establishes a novel mechanism for MOR-mediated protection from intestinal injury and suggests that opioids, which are already widely available clinically, could be used to treat intestinal injury in humans.

of in vivo imaging techniques. Furthermore, the anatomy and physiology of their digestive tract is similar to that of mammals, with a pancreas, liver, gall bladder and intestine (Pack et al., 1996; Ng et al., 2005; Wallace et al., 2005). The zebrafish intestinal epithelium displays proximal-distal functional specification and contains most of same cell lineages found in mammals, including absorptive enterocytes, goblet cells and enteroendocrine cells (Ng et al., 2005; Wallace et al., 2005). The zebrafish digestive tract develops rapidly to permit feeding and digestive function by 5 days post fertilization (dpf). Zebrafish also possess innate and adaptive immune systems homologous to those of mammals (Meeker and Trede, 2008; Kanther and Rawls, 2010). Previous studies have attempted to establish models of intestinal injury in zebrafish larvae by immersion in the hapten 2,4,6-trinitrobenzene sulfonic acid (TNBS) or with the use of the detergent dextran sodium sulfate; however, these models lack overt pathological changes to the intestinal tract based on histology, and the inflammation and injury produced is not intestine-specific (Fleming et al., 2010; Oehlers et al., 2011; Oehlers et al., 2012).

Here, we describe a novel larval zebrafish model of acute intestinal injury using the NSAID glafenine. NSAIDs are known to disrupt the intestinal epithelium, leading to ulceration and inflammation in both humans and in mice (Morteau et al., 2000; Maiden et al., 2005). Additionally, zebrafish have homologs for both cyclooxygenase (COX) isoforms (the targets of NSAIDs) that function similarly and display the same responses to prototypical pharmacological inhibitors as seen in mammals (Grosser et al., 2002). Our work establishes that administration of glafenine larvae for 1-12 hours results in profound intestinal injury, with limited evidence of damage in extra-intestinal locations. Immersion in glafenine resulted in intestinal epithelial cell (IEC) apoptosis and sloughing due to induction of ER stress combined with inhibition of appropriate compensatory UPR responses. In contrast to previous reports of TNBS injury in the zebrafish (Fleming et al., 2010; Oehlers et al., 2011), the glafenine-induced injury model shows profound pathological changes to the intestine and appears to be specific to the gastroenterological system. We demonstrate for the first time that MOR signaling induces the UPR signals to enhance restitution, thereby protecting against glafenine-induced intestinal injury.

RESULTS

Glafenine administration produces cellular sloughing comprising apoptotic IECs

NSAIDs induce gastrointestinal damage in both humans and mice through COX blockade (Morteau et al., 2000; Maiden et al., 2005). In an effort to develop a zebrafish model of gastrointestinal injury, we exposed zebrafish larvae at 5.5 dpf to a panel of NSAIDs for 12 hours (supplementary material Fig. S1A). Administration of Sc-560 (COX-1) (Teraoka et al., 2009), Ns-360 (COX-2) (Grosser et al., 2002) or indomethacin (non-specific) (Grosser et al., 2002) all failed to generate a visible intestinal phenotype, using maximum tolerable dosages that did not result in a rate of death ≥50% (data not shown). Furthermore, combined administration of Sc-560 and Ns-360 resulted in 100% death (data not shown). However, administration of the non-specific NSAID glafenine induced the formation of an opaque, impacted intestinal lumen extending from the distal part of segment 1 through segment 3, with the production of a visible 'tube' of material extending from the cloaca (Fig. 1A, white arrowheads). Dose titration studies revealed that administration of 25 μM glafenine for 12 hours produced the highest level of tube formation with minimal zebrafish death (supplementary material Fig. S1B).

Because of the documented role of prostaglandins in IEC survival (Morteau et al., 2000), we speculated that the impacted lumen was composed of expulsed dead IECs. To test whether cells in the lumenal mass were still alive, we exposed untreated and glafenine-treated zebrafish to the vital dye Acridine Orange (AO) for 30 minutes and imaged them by fluorescence microscopy. An intense streak of AO-positive cells in the lumen of glafenine-exposed fish could be observed by both wide-field and confocal microscopy (Fig. 1B), suggesting the presence of cellular entities. The mass extending from the cloaca observed by brightfield microscopy (Fig. 1A) was also AO-positive, suggesting that dead cells are expelled from the distal intestine through the cloaca. Analysis of relative AO fluorescence in the intestinal lumen revealed a 2.2-fold increase in glafenine-treated fish compared

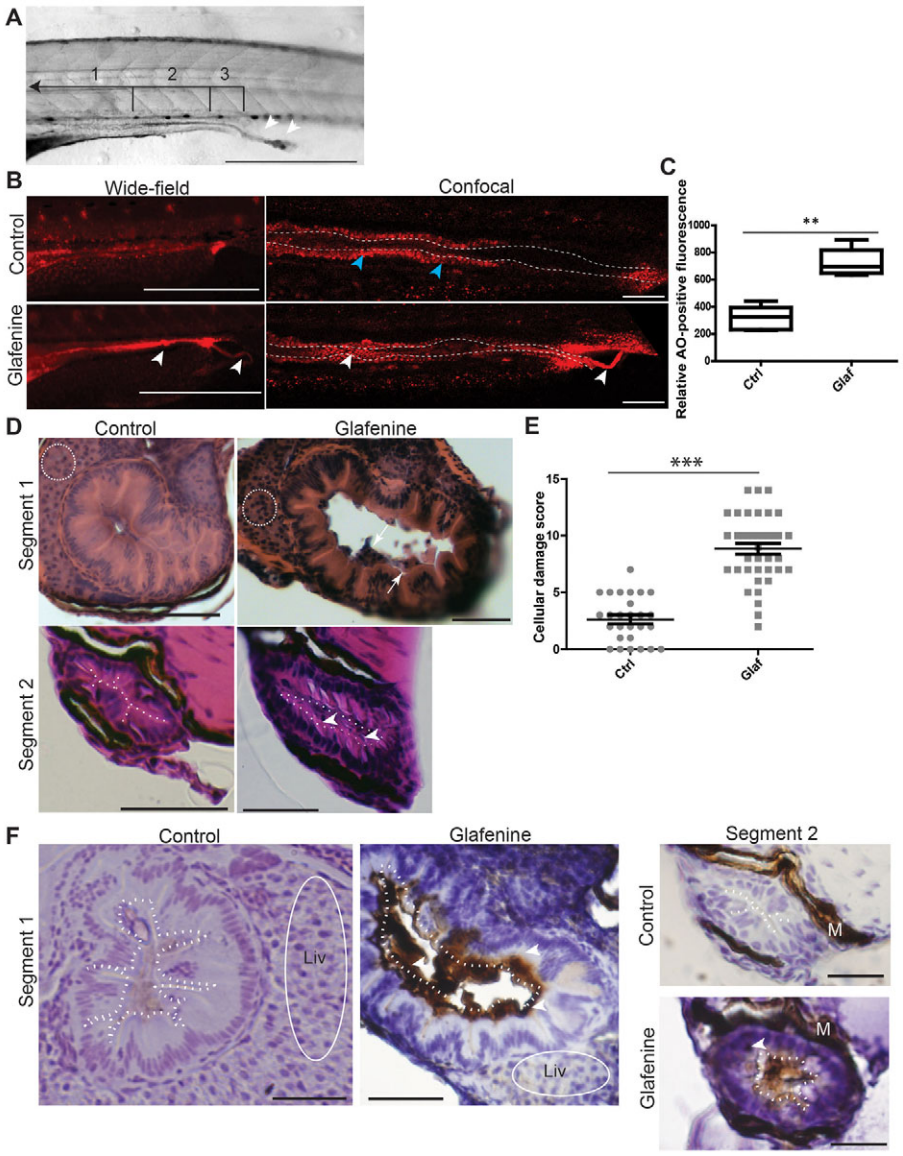

Fig. 1. Glafenine results in apoptotic cell death with sloughing and dysmorphic cellular architecture. (A-F) All studies were made after 12 hours of glafenine exposure in 5 dpf zebrafish. (A) Lumenal sloughing is apparent on brightfield microscopy. Segments 1-3 of the intestine are bracketed and labeled. Arrowheads show sloughing from the intestine. Scale bar: 1 mm. (B) AO staining shows apoptotic lumenal and sloughing debris. Blue arrowheads point to enterocytes that auto-fluoresce red; white arrowheads point to apoptotic lumenal and extruded debris. Scale bars: 1 mm for wide-field images, 50 µm for confocal images. (C) Apoptotic mass can be detected by differences in relative AO fluorescence. Representative of four independent experiments, $n \geq 4$ per experiment. (D) H&E sections showing glafenine-induced injury. Regions of liver are encircled with white dashes (segment 1). The apical surface of the intestinal epithelium is outlined in white (segment 2). Arrows point to sloughed cellular debris and arrowheads point to nuclei. Scale bars: 50 µm. (E) Segment 2 histological scores, pooled from three independent experiments; *n* for each group is indicated on the graph. (F) Activated caspase-3 immunohistochemistry. The apical surface of the intestinal epithelium is outlined in white dots. Regions of liver are encircled by a solid white line. Arrowheads point to positively staining IECs; M, melanocytes; Liv, liver. Scale bars: 50 µm for segment 1, 12.5 µm for segment 2. $^{**}P<0.01$, $^{***}P<0.001$.

with untreated controls (Fig. 1C). Histological assessment of serial sections revealed marked intestinal sloughing into the lumen in segment 1, whereas segment 2 was characterized by an impacted lumen with pyknotic epithelial nuclei, cellular hypertrophy/hyperplasia and apical/sloughing nuclei (Fig. 1D; supplementary material Fig. S2B-E). All of these phenotypes are signs of cellular damage and apoptosis. Blinded, histological scoring of segment 2 sections showed a statistically significant increase in cellular damage in glafenine-treated fish compared with control (8.8 compared with 2.6; Fig. 1E). In addition, an increase in activated caspase-3-positive cells was observed in the epithelium (segment 1) and lumenal debris (segments 1 and 2) of glafenine-treated fish but not untreated fish (Fig. 1F). This staining was not seen using IgG control antibody (supplementary material Fig. S2F). By contrast, caspase-3 staining was virtually absent in the liver of glafenine-treated zebrafish (Fig. 1F, encircled in white). Together, these findings suggest that glafenine treatment induces cellular apoptosis in the intestine.

We next performed kinetic analysis of glafenine-induced intestinal injury. To facilitate this, we developed a rapid assay for apoptosis and/or injury (see Methods) using AO staining. We observed that glafenine induced epithelial injury and apoptotic tubes in about 50% of zebrafish as early as 3 hours, which increased to ~90% of fish after 12 hours of exposure (Fig. 2A). Histological analysis of segment 2 after 3 hours of glafenine exposure confirmed the presence of injured epithelial cells (Fig. 2B). Additionally, marked intestinal sloughing was found in segment 1 after 3 hours (Fig. 2C) and this feature persisted through 12 hours of treatment (Fig. 1D). Histological analysis of the liver after 3, 6 and 12 hours of glafenine exposure showed minimal cellular damage that could be at best described as hydropic changes, maximally seen at 6 hours (Fig. 2D). To determine whether glafenine is still bioactive after long-term treatment (12 hours), media-swapping studies were performed where a new, untreated cohort of zebrafish were introduced into medium in which a different group of zebrafish had been exposed to glafenine for 12 hours. The conditioned media

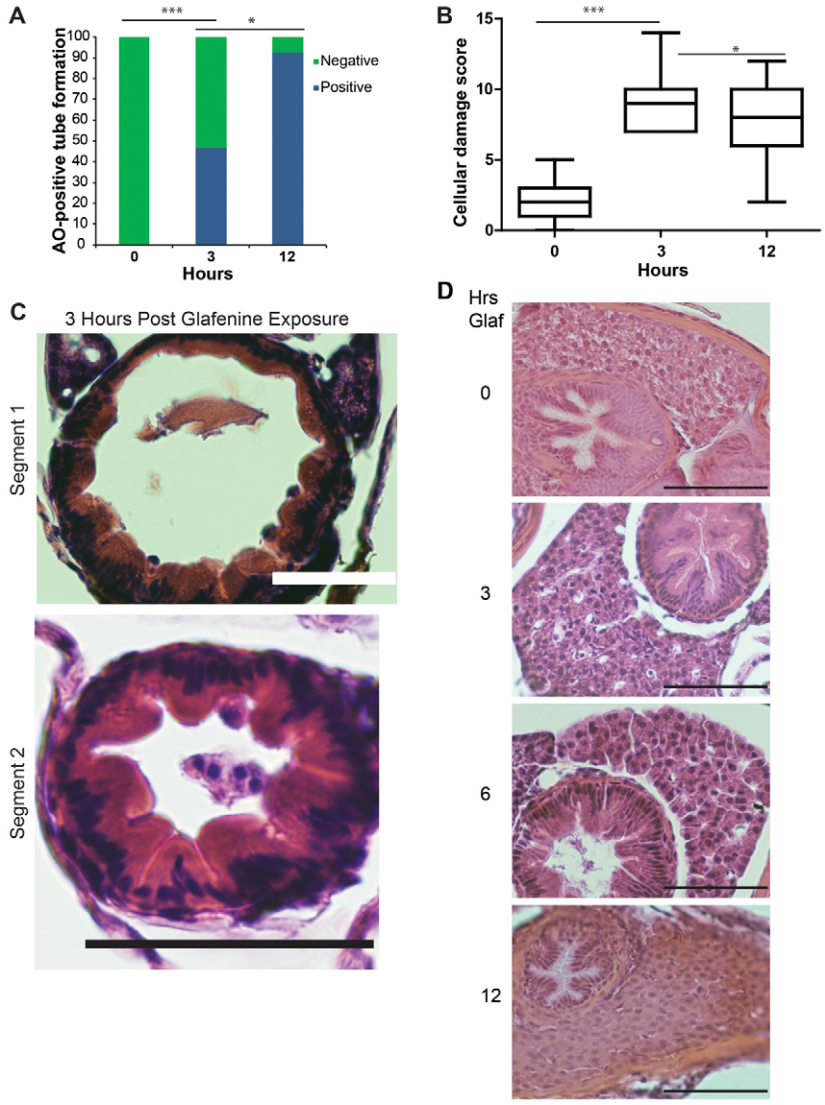

Fig. 2. Progressive glafenine-induced injury over 0-12 hours is centered on the intestine. (A) AO-positive tube formation, $n \geq 13$. (B) Segment 2 histological score, $n \geq 9$. The 0 and 12-hour time points are recapitulated from Fig. 1. (C) Histology at 3 hours. (D) H&E sections of livers of zebrafish exposed to 0, 3, 6 and 12 hours of glafenine. Mild hydropic changes are seen at 6 hours. Scale bars: 50 µm. *P<0.05, ***P<0.001.

did not lead to AO-positive tubes in the new group of fish (data not shown). These data demonstrate that glafenine-induced injury occurs acutely and that the drug is no longer active after 12 hours.

To identify the cellular origins of the damaged cells, we performed transmission electron microscopy (TEM) ultrastructural analysis of glafenine-treated fish. The apoptotic tubes observed macroscopically in glafenine-exposed fish comprised cellular debris and multiple, distinctively apoptotic IECs within the epithelium of segments 1 and 2 and in the lumen of segment 2 (Fig. 3A), confirming that the caspase-3 and AO signals described earlier were due to apoptosis. Debris consistent with microvilli vesiculation, a hallmark of apoptotic cell shedding (Marchiando et al., 2011), was also observed only in injured zebrafish (Fig. 3B). In addition, IECs of glafenine-exposed zebrafish showed features of ER stress with pitted ER in intestinal segments 1 and 2, which was most pronounced after 3 hours of glafenine exposure (Fig. 3C). Further kinetic analysis revealed increasing signs of ER and mitochondrial stress over time, from 1-12 hours of exposure (Fig. 4A,B). Early signs of ER stress peaked at 3 hours, whereas organelle stress (along with apoptosis) steadily increased up to 12 hours after initial exposure; however, despite the fact that restitution of cell stress appeared to be initiated, most organelles were not fully enveloped by membrane, indicating that the cellular stress responses processes were in the early stages (Fig. 4A,B).

To determine whether glafenine-induced IEC apoptosis was associated with reductions in epithelial barrier function, we gavaged zebrafish with Texas Red (TxR)-labeled 10 kD dextran and monitored extra-intestinal fluorescence (Cocchiaro and Rawls, 2012). Strikingly, extra-intestinal fluorescence in zebrafish treated with glafenine for 1 or 3 hours was low and indistinguishable from untreated controls (Fig. 5A,B). By contrast, positive control treatment groups co-gavaged with TxR-dextran and 20 mM EDTA displayed infiltration of TxR-dextran into intersomitic spaces and circulation (Fig. 5A). These results suggest that glafenine treatment alone does not robustly compromise epithelial barrier function during acute damage when the drug is most active. TxR-dextran gavage after 12 hours of glafenine exposure exhibited similar results (data not shown).

Because glafenine has been reported to cause anaphylaxis in humans, as well as liver damage (Stricker et al., 1990; van der Klauw

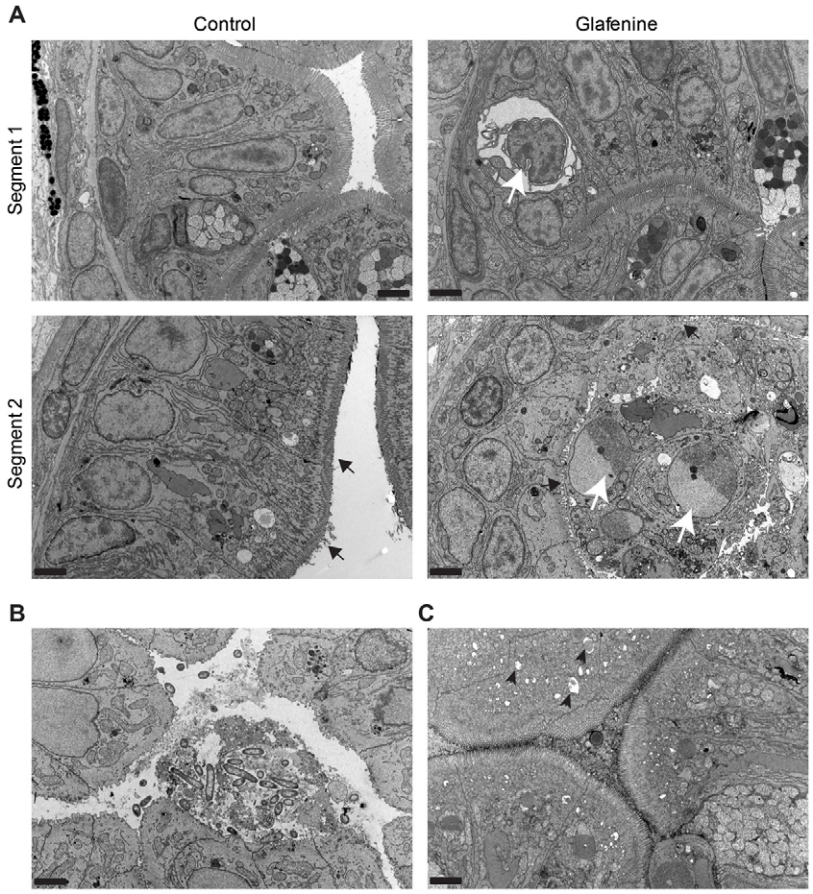

Fig. 3. TEM identifies the apoptotic cells as intestinal epithelial in origin. (A-C) TEM images, representative of two separate fish, across multiple sections after 12 hours of glafenine exposure. 5000× magnification; scale bars: 2 µm. (A,B) Samples fixed after 12 hours of exposure. (C) Images taken after 3 hours of exposure to glafenine. (A) Ultrastructure architecture of control and glafenine-injured fish in segments 1 and 2 of the intestinal epithelium. Apoptotic IECs (white arrow in segment 1) and lumenal cellular debris (white arrows in segment 2) can be observed. Brush border is indicated by black arrows. (B) Lumenal debris seen with glafenine-induced injury in segment 1, which is consistent with microvesiculation of intestinal brush border. (C) ER stress in segment 2, with characteristic pitting marked by black arrowheads.

et al., 1993), we determined the impact of glafenine in extra-intestinal sites. Importantly, no changes were observed in the skin or musculature of glafenine-treated fish, suggesting a predominantly gastrointestinal phenotype (Fig. 6). This was confirmed by AO staining, which revealed no effects of glafenine treatment, except in the liver (Fig. 7). However, histological analysis and caspase-3 staining failed to document evidence of hepatocellular damage or death (Figs 1, 2). Together, these data suggest that glafenine causes minimal liver damage. Additionally, we noticed no gross bleeding into the intestine in control and glafenine-exposed *Tg(gata1:dsRed)*^{sd2};*(kdr1:EGFP)*^{s843} fish, with all dsRed-labeled red blood cells overlapping the EGFP-labeled vasculature (supplementary material Fig. S3A,B). Together, these data suggest a gastrointestinal-specific phenotype, with damage most specific to the intestinal tract.

The µ-opioid agonist DALDA protects against glafenine-induced injury

Because apoptosis is an important feature of our model, we investigated the impact of anti-apoptotic, pro-proliferative, and/or pro-migratory compounds on glafenine-induced injury using the formation of AO-positive tubes as a rapid screening assay. We identified several compounds that conferred protection against glafenine-induced injury when added to the housing medium. R-spondin1 (a β-catenin activator), the MOR agonist DALDA, the COX-2 derivative product dmPGE2 and the pan-caspase inhibitor Q-VD-OPh all afforded significant protection (Fig. 8A). These compounds all share the characteristic of engaging anti-apoptotic or pro-survival signaling pathways (Zhao et al., 2007; Ootani et al., 2009; North et al., 2010; Goldsmith et al., 2011). By contrast, the mitogenic factors human insulin-like growth factor (hIGF1) and mouse epidermal growth factor (mEGF) failed to protect against glafenine-induced injury. Together, these data suggest that only a subset of pro-survival, anti-apoptotic signals are protective in this model. We hypothesized that mitigation of organelle stress was the common factor in the effect of the drugs that reduced glafenine-mediated AO tube formation.

Given the recent discovery of the intestinal-protective effects of µ-opioid signaling (Goldsmith et al., 2011), we decided to further investigate the effect of this opiate on intestinal injury in this zebrafish model. Co-administration of the opioid inhibitor Naloxone (1 mM) alongside DALDA treatment abolished DALDA-mediated protection as determined by the tube assay (data not shown), demonstrating that protection by DALDA was mediated through MOR signaling. Histological assessment of DALDA-treated, glafenine-exposed fish showed a ~45% decrease in intestinal damage compared with untreated glafenine-exposed animals (Fig. 8B). In addition, glafenine-induced zebrafish mortality was improved by about twofold by DALDA treatment (Fig. 8C). Because apoptosis plays a central role in this injury model, we determined the level of activated caspase-3 staining in the intestinal tissues of zebrafish co-treated with glafenine and DALDA. In accordance with

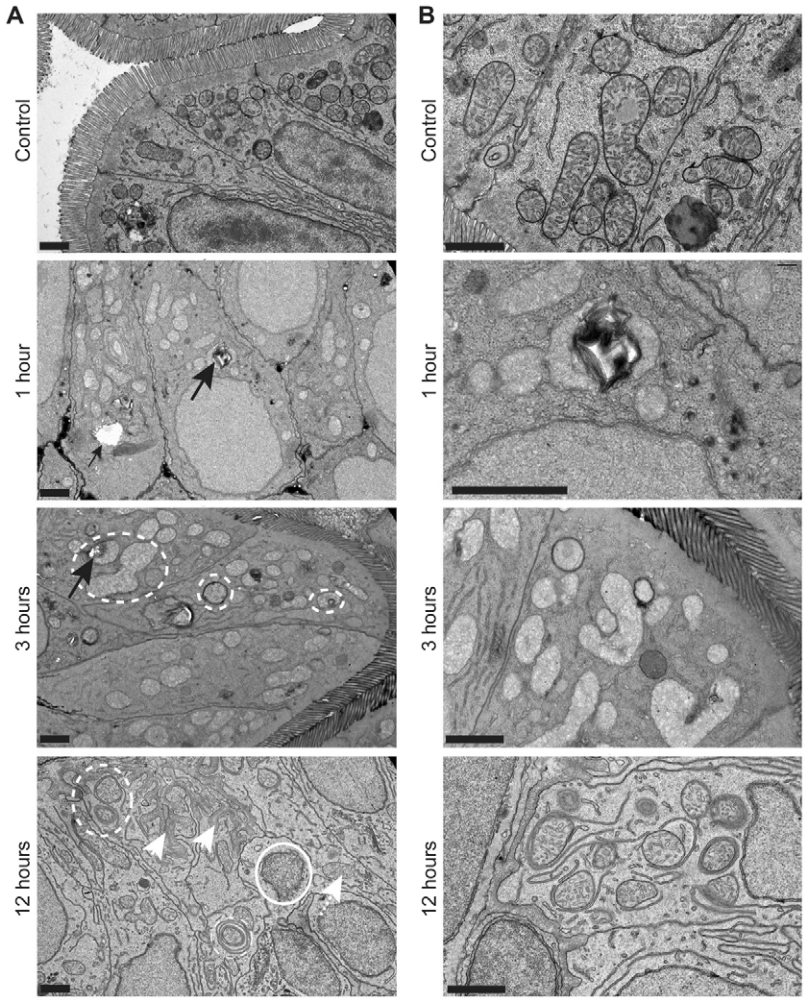

Fig. 4. Glafenine leads to ER stress and arrested cell stress responses. (A,B) Zebrafish larvae at 5.5-6 dpf were exposed to glafenine for the indicated times. Black arrows point to ER stress evidenced by pitting. Dashed circles outline stressed organelles being enveloped by membrane. Solid circles outline dead organelles. White arrowheads point to basement membrane invagination; white arrowhead with dashed line points to stressed mitochondria. Scale bars: 1 μm. (A) Lower magnification images. (B) Higher magnification images.

decreased AO tube formation and improvement of animal survival, DALDA sharply reduced the amount of activated caspase-3 staining in the intestine compared with fish exposed only to glafenine (Fig. 8D). Additionally, DALDA treatment enhanced epithelial cell proliferation during glafenine-induced injury about twofold, as measured by EdU incorporation (Fig. 8E).

Opioid signaling overcomes glafenine-induced blockade of organelle stress response genes, allowing cell survival

Because DALDA amelioration of glafenine-induced intestinal injury is associated with decreased apoptotic markers, we speculated that protection by DALDA is mediated by either preventing the observed organelle stress and/or by increasing compensatory responses such as the UPR that can ward off apoptosis in the presence of cell stress. Interestingly, more organelle stress was present (although diminished) in zebrafish treated with DALDA than with glafenine-induced injury alone (Fig. 9A). DALDA-treated zebrafish maintained an organized epithelium without basement membrane invagination, and organelles did not appear swollen or lacking in sub-organelle architecture. ER stress, as indicated by pitting white lesions, was not prominent in DALDA-treated fish. Also, increased smooth ER and re-establishment of subcellular structures was apparent, presumably the result of resolving cell stress response (Fig. 9A). IECs in the DALDA-treated group also displayed enhanced rough ER (Fig. 9B), a typical sign of resolving cell stress because resolution requires increased protein synthesis.

Given the presence of ER and organelle stress, we investigated the downstream proteins and genes of the UPR cascade. Protein levels of the early UPR mediator BiP were similar in lysates from whole fish exposed to glafenine with or without DALDA (Fig. 9C). By contrast, eIF2a phosphorylation, which is downstream of PERK activation, could not be detected (data not shown). Quantitative RT-PCR assays using microdissected digestive tracts demonstrated that two UPR genes normally upregulated downstream of BiP accumulation, spliced-*xbp1* (*s-xbp1*) and *atf6* (Shen et al., 2005; Cinaroglu et al., 2011), were atypically not upregulated in glafenine-exposed compared with untreated fish, although these genes were induced in DALDA-treated fish (Fig. 9D). These results were recapitulated using whole larvae lysates (supplementary material Fig. S4A), and DALDA was able to drastically induce these genes in the absence of glafenine-induced injury and inhibition (supplementary material Fig. S4B). Because *atf6* is a key mediator of organelle stress responses, leading to the UPR, we next determined the functional role of this gene in DALDA-mediated protection from injury. Zebrafish injected with *atf6*-morpholino (MO) displayed abrogation of DALDA-mediated rescue of

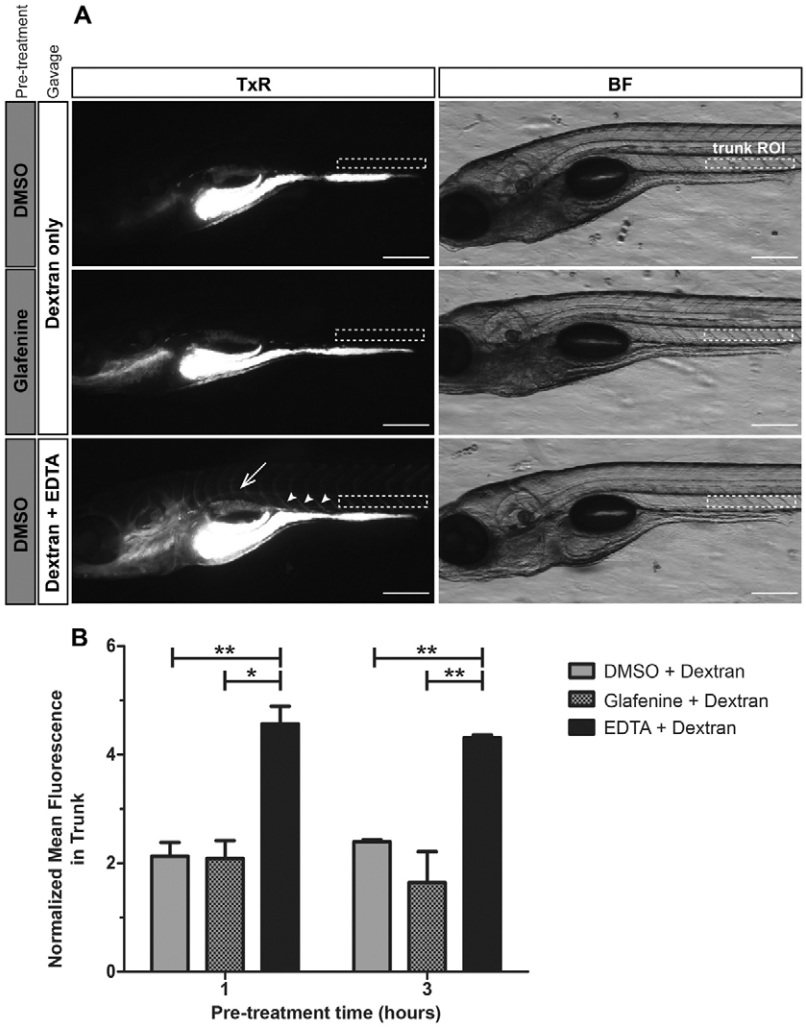

Fig. 5. Intestinal epithelial barrier leakage does not occur with acute glafenine treatment. (A,B) Zebrafish larvae at 6 dpf were pretreated with glafenine or vehicle control for 1 or 3 hours, followed by gavage with 1% TxR-dextran or 1% TxR-dextran plus 20 mM EDTA (positive control). ImageJ was used to quantitate the relative mean fluorescence in an ROI in the zebrafish larvae trunk above segments 2 and 3 of the intestine (white dashed rectangles). Values were normalized to an ROI outside of the fish as an internal control to account for background glare. (A) Dextran leaks into circulation and intersomitic spaces when co-gavaged with EDTA. Representative images of larvae from the 1-hour pretreatment group are shown. In larvae gavaged with dextran only, the dextran remains in the intestinal lumen. When co-gavaged with dextran plus EDTA, fluorescent signal is observed in circulation (dorsal aorta, white arrow) and intersomitic vessels and spaces (white arrowheads). BF, brightfield. Scale bars: 200 µm. (B) Treatment with glafenine does not lead to acute intestinal barrier disruption. Mean normalized fluorescence in the trunk was determined following 1 or 3 hours of pretreatment with glafenine or control. Graph represents data averaged from two experimental replicates taking into account the mean, s.d. and *n* (16-19 larvae/condition/experiment). Two-way ANOVA with Bonferroni post-test was performed to compare each column to all other columns. **P*<0.05, ***P*<0.01.

glafenine-induced injury compared with animals injected with control MO (Fig. 9E), suggesting that enhancement of the UPR response mediates DALDA rescue of glafenine-induced injury.

DISCUSSION

Recent studies in mice and in human patients have implicated improper IEC autophagy and UPR in the face of ER stress as a potential etiology for IBD (Kaser et al., 2008; Kaser et al., 2010; Stappenbeck et al., 2011). In this study, we recapitulate this IEC apoptosis in the zebrafish using the NSAID glafenine, an inhibitor of both COX isoforms that was withdrawn from the market after phase IV studies showed that the drug results in anaphylaxis and gastrointestinal disturbances in human patients (Stricker et al., 1990). Current murine models for studying ER-stress-induced IEC damage require the production of genetic knockouts. This zebrafish model provides several advantages over those systems, including the use of chemical induction and the ease of live imaging and screening for intestinal damage phenotypes. This is also the first larval zebrafish model to demonstrate marked intestinal pathology, namely IEC apoptosis. Previous reports only presented vague systemic inflammatory infiltration without overt changes in the intestinal epithelium (Fleming et al., 2010; Oehlers et al., 2011; Oehlers et al., 2012).

We present several lines of evidence indicating that the NSAID glafenine induces IEC apoptosis by enhancing ER stress, while interfering with compensatory rescue UPR (Fig. 10). First, TEM revealed ER pitting shortly after glafenine exposure (1-3 hours), a hallmark of ER stress. After extended glafenine exposure (12 hours), IECs displayed features that indicated an arrested cell stress response, including partially enveloped organelles and numerous swollen, stressed organelles in living epithelial cells alongside many distinctively apoptotic cells. Secondly, induction of UPR-associated genes *atf6* and *s-xbp1* are impaired in glafenine-exposed fish. Finally, the presence of activated caspase-3-positive apoptotic cells in both intestinal epithelium and the lumenal compartment of glafenine-treated fish are consistent with a failure to adequately respond to cellular stress (Codogno and Meijer, 2005; Kaser et al., 2008; Kaser et al., 2010; Franceschelli et al., 2011). These findings suggest that glafenine induces a strong IEC stress phenotype that translates into increased cellular apoptosis and epithelial damage. Although some liver damage probably exists, the intestinal phenotype is far more pronounced. Additionally, our TEM analysis

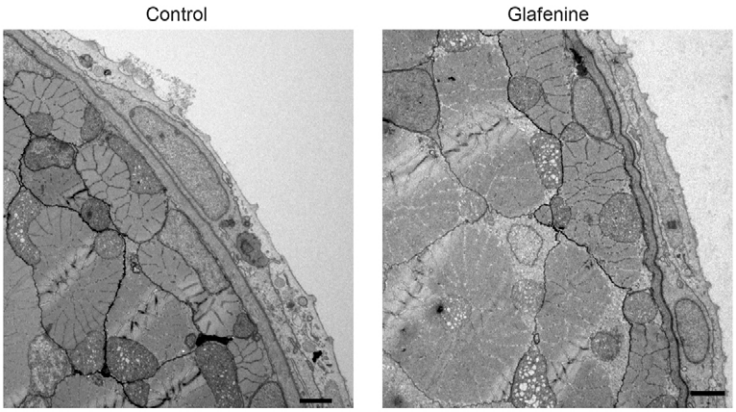

Fig. 6. TEM studies show that glafenine-induced injury keeps the skin and musculature intact. TEM images, representative of three separate fish, after 12 hours of glafenine exposure. 2500× magnification. Scale bars: 2 µm.

and AO staining studies, alongside the use of an NF-κB reporter strain to assess tissue-specific NF-κB activity (supplementary material Fig. S5) (Kanther et al., 2011) showed a gastrointestinal-specific phenotype, another strength of this model.

Interestingly, despite the observed IEC apoptosis, the epithelial barrier remains intact. Using TxR-labeled dextran and oral gavage, we observed that the dextran does not leak out of the intestine in glafenine-treated zebrafish. This suggests that glafenine-induced apoptosis is highly controlled and results in cell shedding with maintenance of the epithelial barrier. Our TEM results support these findings, demonstrating the presence of shedding apoptotic IECs in the epithelial border with maintenance of the barrier by

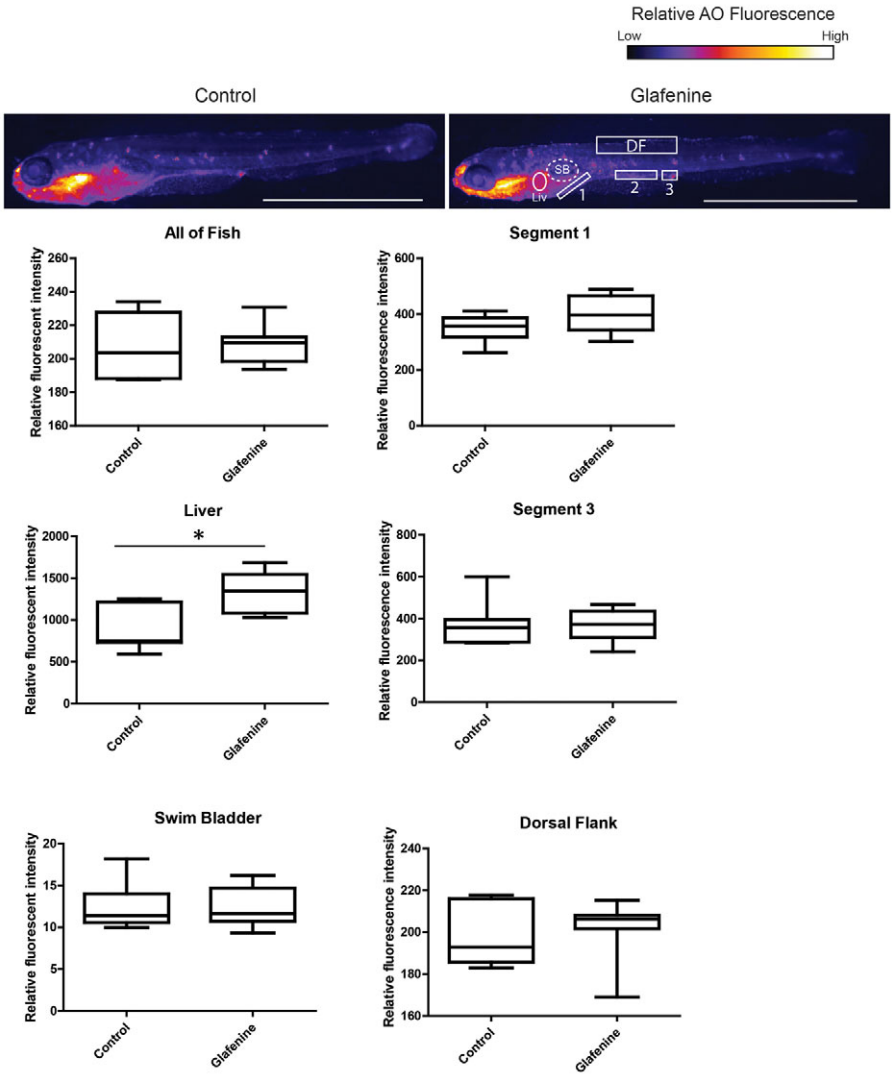

Fig. 7. Glafenine-induced injury is specific to the gastrointestinal system. AO staining marks apoptotic cells throughout the fish. Studies were performed after 12 hours of glafenine exposure. Representative control and glafenine-treated fish are shown, with the regions analyzed shown on the glafenine image. Values are representative of three independent experiments, $n \geq 4$ fish/experiment/condition; *$P<0.05$. SB, swim bladder; Liv, liver; DF, dorsal fin. Scale bars: 1 mm.

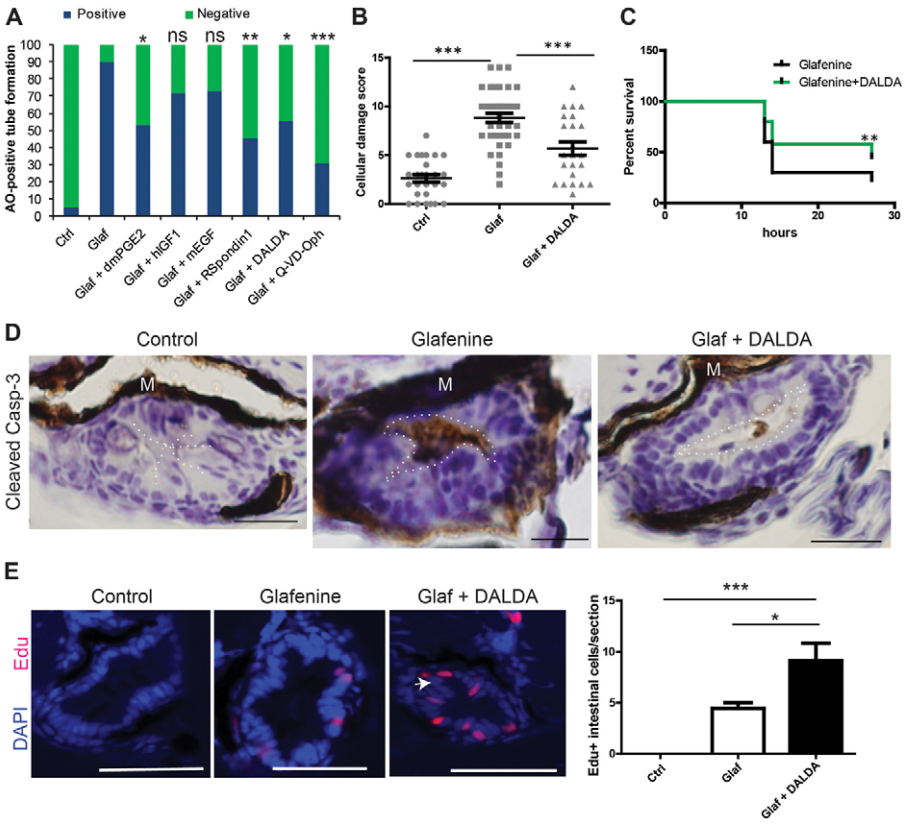

Fig. 8. Glafenine-induced injury can be prevented with a subset of anti-apoptotic and/or pro-survival drugs, including the MOR agonist DALDA. (A-E) All studies performed after 12 hours of drug(s) exposure. (A) Rapid apoptosis assays show that glafenine-induced injury can be prevented by drugs that engage pro-survival and/or anti-apoptotic signaling, but not solely proliferative signalling; $n \geq 15$ per group. Control, glafenine and glafenine + DALDA results are all representative of three or more independent experiments; dmPGE2 results are representative of two independent experiments; other drugs results are representative of replicate experiments performed on the same day with different groups of larvae. Significance shown is relative to glafenine treatment alone; $P<0.001$ between control and glafenine groups (not shown on graph); n for each group is represented on the graph. Dosages: 10 µM dmPGE2, 250 ng/ml hIGF1, 10 nM mEGF and R-spondin, 50 µM Q-VD-Oph. (B) Segment 2 histological scores. Control and glafenine groups are recapitulated from Fig. 1, for ease of comparison with DALDA treatment. (C) DALDA enhances zebrafish survival from glafenine-induced injury. $n=50$, pooled from three independent experiments. Glafenine was used at 50 µM final concentration. (D) Activated caspase-3 immunohistochemistry staining in the intestinal epithelium. Representative of four fish per group. The lumenal edge is outlined in white; M, melanocytes. Scale bars: 12.5 µm. (E) Proliferation in segment 2 in response to drug treatment. White arrow shows hyperplastic cells seen with DALDA administration. Scale bars: 50 µm. Graph shows EdU staining of zebrafish with 12 hours of drug exposure for each group. $n \geq 8$, except for control group, where $n=4$; $^*P<0.05$, $^{**}P<0.01$, $^{***}P<0.001$.

cells basal to the dying cell, together forming the characteristic Y-pattern of controlled cell shedding (Marchiando et al., 2011). Additionally, glafenine treatment of zebrafish larvae has previously been shown to cause increased activity of digestive enzymes phospholipase and protease within the intestinal lumen (Hama et al., 2009). Our results provide a potential physiological explanation for this observation: that these and other enzymes are released promiscuously from apoptotic IECs after glafenine exposure.

Although our kinetic and media-swapping studies suggest that glafenine-induced injury is rapid and acute, the mechanism by which glafenine induces epithelial-specific stress responses and damage is uncertain.

Intestinal epithelium damage is a well-known effect of COX inhibitors (Morteau et al., 2000; Maiden et al., 2005). NSAIDs decouple mitochondrial oxidative phosphorylation within 1 hour of administration (Somasundaram et al., 2000), resulting in ER and general cell stress that in the highly energy-dependent enterocyte can lead to cellular death. In our model, TEM showed characteristic mitochondrial vacuolization typical of NSAID-induced mitochondrial injury, suggesting that this could be the mechanism of injury in our model. Previous, in vitro only, studies demonstrated that other NSAIDs induce apoptosis through improper ER stress responses (Franceschelli et al., 2011), also suggesting that the effects of glafenine observed here are a result of its COX-inhibitory properties. The fact that dmPGE2 rescues zebrafish from IEC apoptosis in this model supports this notion. The observation that other NSAIDs were unable to recapitulate the injury caused by glafenine suggests that these inhibitors, as opposed to glafenine, mainly cause extra-intestinal-mediated mortality over intestinal injury. This is compatible with our observation that zebrafish treated with other NSAIDs died before development of any intestinal apoptosis. In summary, we postulate that IECs are unable to appropriately response to glafenine-induced ER stress and as a result undergo rapid and but orderly apoptosis.

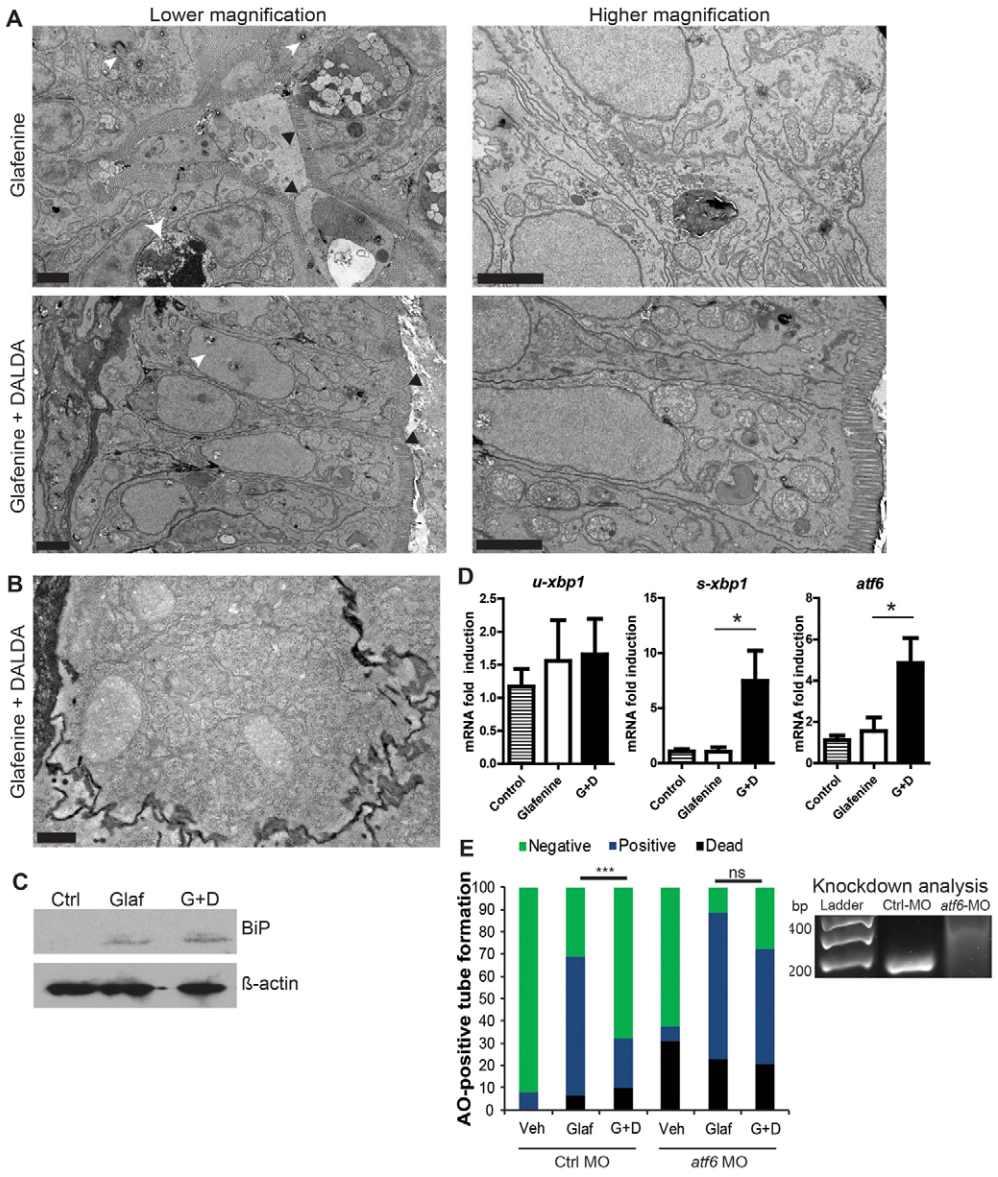

Fig. 9. DALDA reverses glafenine-induced organelle stress and restores proper UPR responses. (A-E) All zebrafish studies were performed after of 12 hours glafenine exposure. (A) TEM with and without DALDA treatment demonstrates a lack of ER and organelle stress and resolved UPR. White arrowheads show pitting from ER stress. White arrow demarks apoptotic IEC. Black arrowheads indicate the brush border. Scale bars: 2 µm. (B) Same conditions as for A, showing granularity in the cytoplasm of segment 1 IECs, indicative of rough ER. Scale bar: 0.5 µm. (C) Glafenine-induced injury causes BiP protein accumulation, an early signal in the UPR cascade. Western blot representative of four independent experiments, each consisting of protein lysate from ≥10 pooled fish per condition. β-actin was used as loading control. (D) Real-time PCR for UPR genes: *u-xbp1* (unspliced), *s-xbp1* (spliced) and *atf6*. Each replicate for each condition was generated from 10 pooled micro-dissected fish gastrointestinal tracts, $n \geq 4$/group. (E) Fish were injected with 5 pmol of control or *atf6* MO in 4.6 nl of water and subjected to the AO tube assay. Values were pooled from two independent experiments, $n \geq 29$/group. veh, vehicle-only group; glaf, glafenine-treated group; G+D, group treated with glafenine plus DALDA. Right: RT-PCR for *atf6* in morpholino-injected fish, at 6 dpf. Wild-type band is at 180 bp, the morphant with an intron-1 inclusion is at 314 bp. Representative of triplicate groups of two independent experiments. $^{*}P<0.05$, $^{***}P<0.001$.

Neuropeptides have attracted interest as a means to modulate intestinal inflammation and to promote epithelial restitution (Philippe et al., 2003). We recently showed that the MOR agonist DALDA protects against DSS-induced intestinal injury through wound healing and proliferative responses in mice (Goldsmith et al., 2011). DALDA promoted intestinal proliferation in glafenine-exposed fish consistent with the previously reported properties of the drug (Goldsmith et al., 2011). However, other zebrafish bioactive proliferative factors (mEGF and hIGF1) (Pozios et al., 2001; Pang and Ge, 2002) failed to prevent glafenine-induced injury, suggesting that proliferation is not the primary protective mechanism of DALDA in this model.

Interestingly, our study identifies a novel means by which µ-opioid signaling might protect against acute epithelial injury. TEM and biochemical analysis of DALDA-treated fish showed decreased organelle stress as well as enhanced UPR, leading to reduced cellular apoptosis and maintenance of epithelial layer integrity. Our studies showed that DALDA enhances *atf6* and *s-xbp1* mRNA expression in zebrafish both in the presence and absence of glafenine, and that the protective effects of DALDA were lost in zebrafish lacking *atf6* function. We therefore conclude that MOR signaling enhances proper cell stress and UPR responses, a previously unknown mechanism of neuropeptide-mediated intestinal protection. At least one important cell stress response pathway, the PI3K pathway (Codogno and Meijer, 2005), is directly activated by MOR signaling (Law et al., 2000), providing a potential mechanism for the action of DALDA in this zebrafish model. To support this hypothesis, addition of the PI3K inhibitor wortmannin resulted in complete loss of DALDA-mediated protection (data not shown). An important consequence of organelle stress is autophagy, which is initiated both downstream of PI3K activation and as a result of the UPR. The role of both systems in our work suggests that glafenine-induced blockade of the UPR could result in diminished autophagy and enhanced cell death, a process reversed by DALDA. Further studies should be pursued to evaluate the role of autophagy in our glafenine system and the effect of DALDA on the autophagic process.

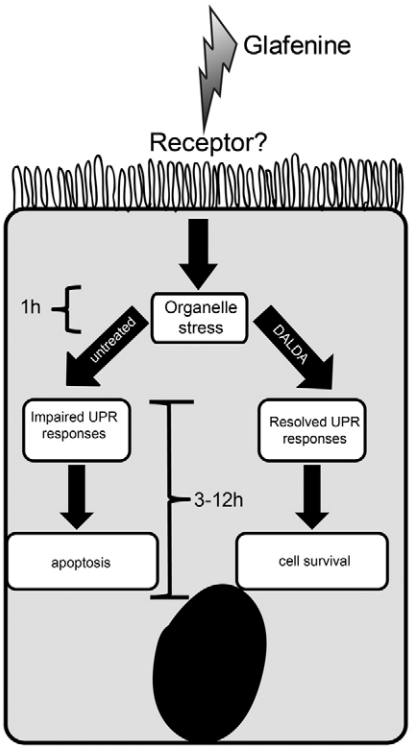

Fig. 10. Schematic of glafenine-induced intestinal injury in zebrafish and MOR-mediated protection. Glafenine induces organelle stress and the UPR response. However, this process is halted with loss of downstream gene induction, leading to inefficient UPR and induction of IEC apoptosis. In the presence of DALDA, glafenine-mediated blockade of the UPR process is restored and autophagy is successfully completed, resulting in reduced IEC apoptosis and maintenance of epithelial layer.

In summary, our findings show that the zebrafish represents a powerful model for the study of cellular and molecular events associated with the intestinal injury response and that human-relevant drugs (DALDA, NSAIDs) have bioactive effects in this vertebrate system. We established a novel zebrafish larvae model of epithelial damage through chemical induction of cell stress and impairment of organelle stress responses. We further demonstrated that the MOR agonist DALDA rescues this intestinal damage by potentiating the appropriate adaptive UPR responses. This novel model of intestinal injury in zebrafish can be utilized to explore the burgeoning field of organelle stress-induced intestinal inflammation and to identify novel targets applicable to human disease.

METHODS

Fish husbandry, zebrafish lines and drugs

All experiments using zebrafish were performed using protocols approved by the Animal Studies Committee of the University of North Carolina at Chapel Hill. Zebrafish were maintained as previously described (Flynn et al., 2009). All experiments were performed on zebrafish at 5.5-6 dpf. Fish were plated into 10-cm diameter Petri dishes, with 20 ml gnotobiotic zebrafish medium (GZM) (Pham et al., 2008), to a maximum of 20 fish/plate the day of the experiment. All drugs (glafenine plus any therapeutics) were administered simultaneously to the water for the indicated period of time. Isovolumetric vehicle controls were used for all experiments. Wild-type TL zebrafish were used for most assays in these studies. Blood flow analysis was performed with *Tg(gata1:dsRed)*^{sd2}*;(kdr1:EGFP)*^{s843} (Traver et al., 2003; Jin et al., 2005) zebrafish. NF-κB activation was assessed with *Tg(NFkB:EGFP)*^{nc1} zebrafish (Kanther et al., 2011). Glafenine (Sigma-Aldrich, St Louis, MO) was dissolved in dimethyl sulfoxide (DMSO), and administered at 25 μM final concentration for all experiments unless otherwise noted. DALDA ([D-Arg2,Lys4]-dermorphin-(1-4)-amide; US Biological; Swampscott, MA) was administered at 10 μM. Indomethacin and Naloxone were obtained from Sigma-Aldrich. Sc-560, Ns-398 and dmPGE2 were obtained from Cayman Chemicals (Ann Arbor, MI); R-spondin1, hIGF1 and mEGF were obtained from R&D Systems (Minneapolis, MN); Q-VD-Oph was obtained from BioVision (Mountain View, CA).

AO tube assay

Fish were submerged in a 1 μg/ml solution of AO (Sigma-Aldrich) and were then anesthetized in 0.017% tricaine and mounted in 3% methylcellulose for visualization using a Leica MZ16F fluorescence stereomicroscope with a dsRed filter. Larvae were scored for the presence of an AO-positive tube extending from the intestine out of the cloaca, or for the presence of a strong red signal in intestinal segment 2. Zebrafish with one of these two characteristics were deemed 'positive'.

Fish imaging and fluorescence quantification

Live zebrafish were anesthetized with 0.017% tricaine (MS-222; Sigma-Aldrich), mounted on 3% methylcellulose and imaged with a Leica MZ16F fluorescence stereomicroscope. Within a given experiment, exposure times and magnifications were held constant. Relative fluorescence intensity was determined with NIH ImageJ (Abramoff et al., 2004), using equal-sized boxes for the region of interest (ROI).

Histology and immunohistochemistry

Larvae were collected and fixed in 4% paraformaldehyde in PBS overnight, then transferred to 70% ethanol for another 24 hours. Fish were then embedded axially in 1% agarose and paraffin embedded. Fish were serially sectioned axially and the distance from the cloaca of each section was established based on section thickness and section number, to determine the section being viewed. We developed a histological scoring system in conjunction with a veterinary pathologist (supplementary material Fig. S2A), using only segment 2 sections due to their more consistent histological presentation. Histological scores were verified by a blinded pathologist.

Immunohistochemistry for activated caspase 3 (R&D Systems) was performed as described (Trotter et al., 2009). 5-Ethynyl-2′-deoxyuridine (EdU) staining was performed using the EdU Click-iT kit (Invitrogen; Carlsbad, CA), according to manufacturer's protocol, with a final EdU concentration of 15 μg/ml. Fish were exposed to EdU for the same duration as glafenine and any other treatments (12 hours). Brightfield histological images were taken on an Olympus IX70 (Olympus; Center Valley, PA) with the default Olympus DP Controller software. An Olympus UpLan Fl 40×, 0.75 NA objective

was used. For fluorescence images, a Zeiss 710 microscope with an oil immersion, 40×, 1.4 NA objective was used (Carl Zeiss; Thornwood, NY). Zeiss Zen 2009 software was used for image acquisition. All images were acquired at room temperature.

Electron microscopy

Zebrafish were collected, euthanized with tricaine (0.083%), and immersion-fixed in 2% formaldehyde, 2.5% glutaraldehyde, 0.1 M sodium cacodylate buffer, pH 7.4, overnight to several days at 4°C. Following post-fixation for 1 hour in potassium ferrocyanide-reduced osmium (Russell and Burguet, 1977), specimens were dehydrated through a graded series of ethanol and embedded in Polybed 812 epoxy resin (Polysciences, Warrington, PA). Transverse 1-µm sections were cut at several locations along the gut, stained with 1% toluidine blue and 1% sodium borate and examined by light microscopy to confirm the ROI. Ultrathin sections were cut with a diamond knife (70-80 nm thickness), mounted on 200 mesh copper grids and stained with 4% aqueous uranyl acetate for 15 minutes followed by Reynolds' lead citrate for 8 minutes (Reynolds, 1963). The sections were analyzed using a LEO EM-910 transmission electron microscope (Carl Zeiss SMT, Peabody, MA), operating at an accelerating voltage of 80 kV. Digital images were taken using a Gatan Orius SC 1000 CCD Camera and DigitalMicrograph 3.11.0 software (Gatan, Pleasanton, CA). All images were acquired at room temperature.

Oral micro-gavage and barrier function assay

Wild-type TL zebrafish larvae at 6 dpf were pretreated in a Petri dish containing 20 ml of GZM plus 0.1 mM phenylthiourea (PTU; to inhibit melanin synthesis) with glafenine (25 µM) or the equivalent amount of the DMSO vehicle control (0.025% v/v) for 1 or 3 hours at 25°C. Following treatment, larvae were gavaged as previously described (Cocchiaro and Rawls, 2012) with 1% TxR-dextran (10,000 molecular weight, D1863; Invitrogen/Molecular Probes) or 1% TxR-dextran plus 20 mM EDTA (positive control). Briefly, larvae were anesthetized in 0.026% tricaine and mounted in 3% methylcellulose layered on an agarose injection mold to position the larvae for gavage and hold them gently in place. Borosilicate glass capillary needles specifically designed for gavage were clipped as bluntly as possible. Using a Drummond Nanoject II microinjection apparatus and stereomicroscope, gavage needles were carefully manoeuvred into the mouths of anesthetized larvae, through the esophagus, and just inside the anterior bulb of the intestine by gently depressing the esophageal sphincter. The dextran gavage solution (4.6 nl on the slow setting) was administered into the anterior bulb. Following gavage, fish were moved to fresh GZM-medium, washed gently to remove methylcellulose, and revived from anesthesia. At 15-20 minutes post-gavage, larvae were re-anesthetized, mounted in 3% methylcellulose on top of a 3% agarose block (to reduce reflection glare) and imaged on a Leica M205C fluorescence stereomicroscope. The same magnification and gain settings were used for all images. ImageJ software was used to quantitate mean relative fluorescence in an ROI in the larvae trunk above the posterior intestine (trunk ROI) and an ROI outside of the fish (background ROI). To ensure consistency in measurement, the posterior side of the trunk ROI was always aligned with the end of cloaca just above the intestine. GraphPad Prism 5.0 was used for graphs and statistical analysis. The assay was also performed for larvae pretreated for longer at 12-14 hours (data not shown).

RT-PCR

Total RNA was isolated from either whole zebrafish larvae or microdissected digestive tracts using an Ambion Purelink Kit (Invitrogren) according to manufacturer's protocol and RT-PCR was performed as described (Kanther et al., 2011) using a ABI Prism HT7700. Specificity and linearity of amplification for each primer set was determined by melting curve analysis and calculation of the slope from serial diluted samples. Relative fold-changes were determined using the ΔΔCT calculation method. Values were normalized to the internal control 18S RNA. Primers: *atf6* (5′-CTGTGGTGAAACCTCCACCT-3′ and 5′-CATGGTGACCA-CAGGAGATG-3′), *xbp1* (5′-GGGTTGGATACCTTGGAAA-3′ and 5′-AGGGCCAGGGCTGTGAGTA-3′), *xbp1-s* (5′-TGTTGCGAGACAAGACGA-3′ and 5′-CCTGCAC-CTGCTGCGGACT-3′), *18S* (5′-CACTTGTCCCTCT-AAGAAGTTGCA-3′ and 5′-GGTTGATTCCGATAACG-AACGA-3′) were previously described (Cinaroglu et al., 2011; Kanther et al., 2011). PCR for analysis of *atf6* morpholino efficacy was performed using specific primers for *atf6* (5′-TAGCCTACACTTTTCACCAG-3′ and 5′-ATGTCGTCG-AATTTAATGTTAG-3′) and the final products visualized on 3% agarose gel (Cinaroglu et al., 2011).

Morpholino knockdown

Zebrafish embryos at the 1- to 2-cell stage were injected with splice-blocking MOs (GeneTools LLC) targeting *atf6* (4.6 pmol/embryo, GAGTGGGGTAAGATACACGTTCTAG; generously provided by Kirsten Sadler Edepli, Mount Sinai School of Medicine); or standard control MO (4.6 pmol/embryo; Gene Tools LLC) using a Drummond Nanoject II microinjector. Efficacy of *atf6* knockdown was measured by RT-PCR.

Protein isolation and western blot analysis

Whole 6-dpf zebrafish were euthanized with 0.083% tricaine and homogenized for 15 seconds with a Polytron in 200 µl cold RIPA buffer containing proteinase inhibitors (Complete Mini; Roche Diagnostics, Penzberg, Germany), phosphatase inhibitor cocktail 2 at a 1:100 dilution (Sigma-Aldrich) and 1 mM phenylmethanesulfonyl fluoride (PMSF; Sigma-Aldrich). Afterwards, lysates were diluted 1:1 with 2× Laemmli buffer. Proteins (30 µg, quantified by Bradford assay) were separated using 10% SDS-PAGE and transferred to nitrocellulose membranes. Blots were then probed with antibodies to BiP (1:3000; Sigma-Aldrich) and β-actin (1:1000; MP Biomedical; Solon, OH). Antibodies were diluted in 5% dry milk in 0.1% Tris-buffered saline containing Tween-20 (TBST). Blots were then washed three times for 5 minutes in the 5% milk-TBST solution and then incubated with an appropriate horse-radish-peroxidase-conjugated secondary antibody (1:5000; GE Healthcare, Piscataway, NJ) for 30 minutes. Proteins were detected by chemiluminescence.

Statistical analyses

Statistical analyses were performed using GraphPad PRISM version 5.0 (GraphPad, La Jolla, CA). Assessments between groups of fish

were done with a two-way analysis of variance (ANOVA). Histology post-tests and further comparisons made between zebrafish were analyzed using a Mann-Whitney U-test at a 95% confidence interval, unless otherwise noted in the figure legend. Relative fluorescence data and EdU cell counting were compared with Student's *t*-tests, at a 95% confidence interval. All graphs depict mean ± s.e.m. Experiments were considered statistically significant if $P<0.05$. For all figures $^{*}P<0.05$, $^{**}P<0.01$ and $^{***}P<0.001$, unless otherwise noted.

ACKNOWLEDGEMENTS

The authors are grateful to Edward Flynn (UNC-CH) for superb technical support; to the Microscopy Services Laboratory of UNC-CH and Victoria Madden for TEM; to Kirsten Sadler Edepli (Mount Sinai School of Medicine) for providing the *atf6* morpholino and technical advice on loading controls; and to Arlin Rogers of the Department of Pathology (UNC-CH) for help developing the histological scoring system.

COMPETING INTERESTS

The authors declare that they do not have any competing or financial interests.

AUTHOR CONTRIBUTIONS

J.R.G., J.L.C., J.F.R. and C.J. conceived and designed the experiments. J.R.G. and J.L.C. performed the experiments. J.R.G., J.L.C., J.F.R. and C.J. analyzed the data. J.R.G., J.F.R. and C.J. wrote the manuscript and J.L.C. edited the manuscript.

FUNDING

This work was funded by the National Institutes of Health [grant numbers R01DK047700 and R01DK073338 to C.J., R01DK081426 to J.F.R., F32DK094592 to J.L.C. and F30DK085906 to J.R.G.].

SUPPLEMENTARY MATERIAL

Supplementary material for this article is available at http://dmm.biologists.org/lookup/suppl/doi:10.1242/dmm.009852/-/DC1

REFERENCES

Abramoff, M., Magelhaes, P. and Ram, S. (2004). Image Processing with ImageJ. *Biophotonics International* **11**, 36-42.

Cinaroglu, A., Gao, C., Imrie, D. and Sadler, K. C. (2011). Activating transcription factor 6 plays protective and pathological roles in steatosis due to endoplasmic reticulum stress in zebrafish. *Hepatology* **54**, 495-508.

Cocchiaro, J. L. and Rawls, J. F. (2012). Microgavage of zebrafish larvae. *J. Vis. Exp.* (in press).

Codogno, P. and Meijer, A. J. (2005). Autophagy and signaling: their role in cell survival and cell death. *Cell Death Differ.* **12 Suppl. 2**, 1509-1518.

Fleming, A., Jankowski, J. and Goldsmith, P. (2010). In vivo analysis of gut function and disease changes in a zebrafish larvae model of inflammatory bowel disease: a feasibility study. *Inflamm. Bowel Dis.* **16**, 1162-1172.

Flynn, E. J., 3rd, Trent, C. M. and Rawls, J. F. (2009). Ontogeny and nutritional control of adipogenesis in zebrafish (Danio rerio). *J. Lipid Res.* **50**, 1641-1652.

Franceschelli, S., Moltedo, O., Amodio, G., Tajana, G. and Remondelli, P. (2011). In the Huh7 hepatoma cells diclofenac and indomethacin activate differently the unfolded protein response and induce ER stress apoptosis. *Open Biochem. J.* **5**, 45-51.

Goldsmith, J. R., Uronis, J. M. and Jobin, C. (2011). Mu opioid signaling protects against acute murine intestinal injury in a manner involving Stat3 signaling. *Am. J. Pathol.* **179**, 673-683.

Grosser, T., Yusuff, S., Cheskis, E., Pack, M. A. and FitzGerald, G. A. (2002). Developmental expression of functional cyclooxygenases in zebrafish. *Proc. Natl. Acad. Sci. USA* **99**, 8418-8423.

Hama, K., Provost, E., Baranowski, T. C., Rubinstein, A. L., Anderson, J. L., Leach, S. D. and Farber, S. A. (2009). In vivo imaging of zebrafish digestive organ function using multiple quenched fluorescent reporters. *Am. J. Physiol. Gastrointest. Liver Physiol.* **296**, G445-G453.

Jin, S. W., Beis, D., Mitchell, T., Chen, J. N. and Stainier, D. Y. (2005). Cellular and molecular analyses of vascular tube and lumen formation in zebrafish. *Development* **132**, 5199-5209.

Kanther, M. and Rawls, J. F. (2010). Host-microbe interactions in the developing zebrafish. *Curr. Opin. Immunol.* **22**, 10-19.

Kanther, M., Sun, X., Mühlbauer, M., Mackey, L. C., Flynn, E. J., 3rd, Bagnat, M., Jobin, C. and Rawls, J. F. (2011). Microbial colonization induces dynamic temporal and spatial patterns of NF-κB activation in the zebrafish digestive tract. *Gastroenterology* **141**, 197-207.

Karrasch, T. and Jobin, C. (2008). NF-kappaB and the intestine: friend or foe? *Inflamm. Bowel Dis.* **14**, 114-124.

Karrasch, T. and Jobin, C. (2009). Wound healing responses at the gastrointestinal epithelium: a close look at novel regulatory factors and investigative approaches. *Z. Gastroenterol.* **47**, 1221-1229.

Kaser, A., Lee, A. H., Franke, A., Glickman, J. N., Zeissig, S., Tilg, H., Nieuwenhuis, E. E., Higgins, D. E., Schreiber, S., Glimcher, L. H. et al. (2008). XBP1 links ER stress to intestinal inflammation and confers genetic risk for human inflammatory bowel disease. *Cell* **134**, 743-756.

Kaser, A., Martínez-Naves, E. and Blumberg, R. S. (2010). Endoplasmic reticulum stress: implications for inflammatory bowel disease pathogenesis. *Curr. Opin. Gastroenterol.* **26**, 318-326.

Kim, J. W. and Jobin, C. (2010). Nod2/GSK3b signaling protects the small intestine against ischemia-reperfusion induced injury in mice. *Gastroenterology* **138 Suppl. 1**, S35.

Kinross, J., Warren, O., Basson, S., Holmes, E., Silk, D., Darzi, A. and Nicholson, J. K. (2009). Intestinal ischemia/reperfusion injury: defining the role of the gut microbiome. *Biomark. Med.* **3**, 175-192.

Law, P.-Y., Wong, Y. H. and Loh, H. H. (2000). Molecular mechanisms and regulation of opioid receptor signaling. *Annu. Rev. Pharmacol. Toxicol.* **40**, 389-430.

Maiden, L., Thjodleifsson, B., Theodors, A., Gonzalez, J. and Bjarnason, I. (2005). A quantitative analysis of NSAID-induced small bowel pathology by capsule enteroscopy. *Gastroenterology* **128**, 1172-1178.

Marchiando, A. M., Shen, L., Graham, W. V., Edelblum, K. L., Duckworth, C. A., Guan, Y., Montrose, M. H., Turner, J. R. and Watson, A. J. (2011). The epithelial barrier is maintained by in vivo tight junction expansion during pathologic intestinal epithelial shedding. *Gastroenterology* **140**, 1208-1218.

Meeker, N. D. and Trede, N. S. (2008). Immunology and zebrafish: spawning new models of human disease. *Dev. Comp. Immunol.* **32**, 745-757.

Morteau, O., Morham, S. G., Sellon, R., Dieleman, L. A., Langenbach, R., Smithies, O. and Sartor, R. B. (2000). Impaired mucosal defense to acute colonic injury in mice lacking cyclooxygenase-1 or cyclooxygenase-2. *J. Clin. Invest.* **105**, 469-478.

Ng, A. N., de Jong-Curtain, T. A., Mawdsley, D. J., White, S. J., Shin, J., Appel, B., Dong, P. D., Stainier, D. Y. and Heath, J. K. (2005). Formation of the digestive system in zebrafish: III. Intestinal epithelium morphogenesis. *Dev. Biol.* **286**, 114-135.

North, T. E., Babu, I. R., Vedder, L. M., Lord, A. M., Wishnok, J. S., Tannenbaum, S. R., Zon, L. I. and Goessling, W. (2010). PGE2-regulated wnt signaling and N-acetylcysteine are synergistically hepatoprotective in zebrafish acetaminophen injury. *Proc. Natl. Acad. Sci. USA* **107**, 17315-17320.

Oehlers, S. H., Flores, M. V., Okuda, K. S., Hall, C. J., Crosier, K. E. and Crosier, P. S. (2011). A chemical enterocolitis model in zebrafish larvae that is dependent on microbiota and responsive to pharmacological agents. *Dev. Dyn.* **240**, 288-298.

Oehlers, S. H., Flores, M. V., Hall, C. J., Crosier, K. E. and Crosier, P. S. (2012). Retinoic acid suppresses intestinal mucus production and exacerbates experimental enterocolitis. *Dis. Model. Mech.* **5**, 457-467.

Ootani, A., Li, X., Sangiorgi, E., Ho, Q. T., Ueno, H., Toda, S., Sugihara, H., Fujimoto, K., Weissman, I. L., Capecchi, M. R. et al. (2009). Sustained in vitro intestinal epithelial culture within a Wnt-dependent stem cell niche. *Nat. Med.* **15**, 701-706.

Pack, M., Solnica-Krezel, L., Malicki, J., Neuhauss, S. C., Schier, A. F., Stemple, D. L., Driever, W. and Fishman, M. C. (1996). Mutations affecting development of zebrafish digestive organs. *Development* **123**, 321-328.

Packey, C. D. and Ciorba, M. A. (2010). Microbial influences on the small intestinal response to radiation injury. *Curr. Opin. Gastroenterol.* **26**, 88-94.

Pang, Y. and Ge, W. (2002). Epidermal growth factor and TGFalpha promote zebrafish oocyte maturation in vitro: potential role of the ovarian activin regulatory system. *Endocrinology* **143**, 47-54.

Pham, L. N., Kanther, M., Semova, I. and Rawls, J. F. (2008). Methods for generating and colonizing gnotobiotic zebrafish. *Nat. Protoc.* **3**, 1862-1875.

Philippe, D., Dubuquoy, L., Groux, H., Brun, V., Chuoï-Mariot, M. T., Gaveriaux-Ruff, C., Colombel, J. F., Kieffer, B. L. and Desreumaux, P. (2003). Anti-inflammatory properties of the mu opioid receptor support its use in the treatment of colon inflammation. *J. Clin. Invest.* **111**, 1329-1338.

Pozios, K. C., Ding, J., Degger, B., Upton, Z. and Duan, C. (2001). IGFs stimulate zebrafish cell proliferation by activating MAP kinase and PI3-kinase-signaling pathways. *Am. J. Physiol. Regul. Integr. Comp. Physiol.* **280**, R1230-R1239.

Reynolds, E. S. (1963). The use of lead citrate at high pH as an electron-opaque stain in electron microscopy. *J. Cell Biol.* **17**, 208-212.

Russell, L. and Burguet, S. (1977). Ultrastructure of leydig cells as revealed by secondary tissue treatment with a ferrocyanide-osmium mixture. *Tissue Cell* **9**, 751-766.

Sartor, R. B. (2008). Microbial influences in inflammatory bowel diseases. *Gastroenterology* **134**, 577-594.

Shen, J., Snapp, E. L., Lippincott-Schwartz, J. and Prywes, R. (2005). Stable binding of ATF6 to BiP in the endoplasmic reticulum stress response. *Mol. Cell. Biol.* **25**, 921-932.

Somasundaram, S., Sigthorsson, G., Simpson, R. J., Watts, J., Jacob, M., Tavares, I. A., Rafi, S., Roseth, A., Foster, R., Price, A. B. et al. (2000). Uncoupling of intestinal mitochondrial oxidative phosphorylation and inhibition of cyclooxygenase are required for the development of NSAID-enteropathy in the rat. *Aliment. Pharmacol. Ther.* **14**, 639-650.

Stappenbeck, T. S., Rioux, J. D., Mizoguchi, A., Saitoh, T., Huett, A., Darfeuille-Michaud, A., Wileman, T., Mizushima, N., Carding, S., Akira, S. et al. (2011). Crohn disease: a current perspective on genetics, autophagy and immunity. *Autophagy* **7**, 355-374.

Stricker, B. H., de Groot, R. R. and Wilson, J. H. (1990). Anaphylaxis to glafenine. *Lancet* **336**, 943-944.

Teraoka, H., Kubota, A., Dong, W., Kawai, Y., Yamazaki, K., Mori, C., Harada, Y., Peterson, R. E. and Hiraga, T. (2009). Role of the cyclooxygenase 2-thromboxane pathway in 2,3,7,8-tetrachlorodibenzo-p-dioxin-induced decrease in mesencephalic vein blood flow in the zebrafish embryo. *Toxicol. Appl. Pharmacol.* **234**, 33-40.

Traver, D., Paw, B. H., Poss, K. D., Penberthy, W. T., Lin, S. and Zon, L. I. (2003). Transplantation and in vivo imaging of multilineage engraftment in zebrafish bloodless mutants. *Nat. Immunol.* **4**, 1238-1246.

Trotter, A. J., Parslow, A. C. and Heath, J. K. (2009). Morphologic analysis of the zebrafish digestive system. *Methods Mol. Biol.* **546**, 289-315.

van der Klauw, M. M., Stricker, B. H., Herings, R. M., Cost, W. S., Valkenburg, H. A. and Wilson, J. H. (1993). A population based case-cohort study of drug-induced anaphylaxis. *Br. J. Clin. Pharmacol.* **35**, 400-408.

Wallace, K. N., Akhter, S., Smith, E. M., Lorent, K. and Pack, M. (2005). Intestinal growth and differentiation in zebrafish. *Mech. Dev.* **122**, 157-173.

Williams, K. L., Fuller, C. R., Dieleman, L. A., DaCosta, C. M., Haldeman, K. M., Sartor, R. B. and Lund, P. K. (2001). Enhanced survival and mucosal repair after dextran sodium sulfate-induced colitis in transgenic mice that overexpress growth hormone. *Gastroenterology* **120**, 925-937.

Wirtz, S., Neufert, C., Weigmann, B. and Neurath, M. F. (2007). Chemically induced mouse models of intestinal inflammation. *Nat. Protoc.* **2**, 541-546.

Zhao, J., de Vera, J., Narushima, S., Beck, E. X., Palencia, S., Shinkawa, P., Kim, K.-A., Liu, Y., Levy, M. D., Berg, D. J. et al. (2007). R-spondin1, a novel intestinotrophic mitogen, ameliorates experimental colitis in mice. *Gastroenterology* **132**, 1331-1343.